

Structure and Characterization of *Eriphia verrucosa* Hemocyanin

A. Dolashki¹ · M. Radkova² · E. Todorovska² · M. Ivanov² · S. Stevanovic³ · L. Molin⁴ · P. Traldi⁴ · W. Voelter⁵ · P. Dolashka¹

Received: 4 February 2015 / Accepted: 25 May 2015
© Springer Science+Business Media New York 2015

Abstract Arthropod hemocyanins (Hcs) are a family of large extracellular oxygen-transporting proteins with high molecular mass and hexameric or multi-hexameric molecular assembly. This study reports for the first time the isolation and characterization of the structure of an arthropod hemocyanin from crab *Eriphia verrucosa* (EvH) living in the Black Sea. Its oligomeric quaternary structure is based on different arrangements of a basic 6×75 kDa hexameric unit, and four of them (EvH1, EvH2, EvH3, and EvH4) were identified using ion-exchange chromatography. Subunit 3 (EvH3) shows high similarity scores (75.0, 87.5, 91.7, and 75.0 %, respectively) by comparison of the N-terminal sequence of subunit 1 from *Cancer pagurus* of the North Sea (Cp1), subunits 3 and 6 of *Cancer magister* (Cm3 and Cm6), and subunit 2 of *Carcinus aestuarii* (CaSS2), respectively. Moreover, a partial cDNA sequence (1309 bp) of *E. verrucosa* hemocyanin encoding a protein of 435 amino acids was isolated. The deduced amino acid sequence shows a high degree of similarity with subunits 3, 4, 5, and 6 of *C. magister* (81–84 %). Most of the hemocyanins are glycosylated, and three putative O-linkage sites were identified in the partial amino acid sequence

of EvH at positions 444–446, 478–480, and 547–549, respectively. The higher stability of native Hc in comparison to its subunit EvH4 as determined by circular dichroism (CD) could be explained with the formation of a stabilizing quaternary structure.

Keywords *Eriphia verrucosa* hemocyanin · cDNA sequence · Quaternary structures · Glycosylation sites

Introduction

Hemocyanins are copper-containing respiratory proteins, dissolved in concentrations up to 120 mg/ml in the hemolymph of molluscs and arthropods, including Crustacea, Chelicerata, Myriapoda, and some species of insects (Hagner-Holler et al. 2004; Sánchez et al. 1998; van Holde and Miller 1995; Chen et al. 2007; Mičetić et al. 2010). These molecules are composed of a number of subunits that assemble in an extremely large macro-molecular entity. These particles, which are similar in size to viruses or ribosomes, exhibit a complex allosteric behavior during oxygen binding.

Arthropod hemocyanins, hexamers, or oligo-hexameric assemblies with a molecular mass from 0.45×10^6 to 3.9×10^6 daltons are cubical molecules which in the electron microscope differ largely from cylindrical particles found in mollusks. Molluscan hemocyanins are decamers, didecamers, or multidecamers of polypeptides of M_r up to 450 kDa that carry seven or eight binuclear copper sites. In contrast, arthropod hemocyanins are hexamers (1×6) or oligohexamers ($n \times 6$), and their aggregates are composed of 6 subunits (Herskovits 1988) with an M_r of 67–90 kDa, each containing only a single copper dioxygen-binding site (Herskovits 1988). Recently, the structures of several arthropod hemocyanins

✉ P. Dolashka
pda54@abv.bg

¹ Institute of Organic Chemistry with Centre of Phytochemistry, Bulgarian Academy of Sciences, G. Bonchev str. 9, Sofia 1113, Bulgaria

² AgroBioInstitute, 8 Dragan Tsankov, Str., 1164 Sofia, Bulgaria

³ Institute for Cell Biology, Department of Immunology, University of Tübingen, Auf der Morgenstelle 15, D-72076 Tübingen, Germany

⁴ CNR-ISTM, Corso Stati Uniti 4, 35129 Padova, Italy

⁵ Interfaculty Institute of Biochemistry, University of Tübingen, Hoppe-Seyler-Str. 4, D-72076 Tübingen, Germany

were very well described (Martin et al. 2007; Cong et al. 2009; Jaenicke et al. 2012; Kölsch et al. 2013).

Amino acid sequences of some isoforms of hemocyanins from several arthropod species have also been determined: subunits a, b, and c of *Panulirus interruptus* hemocyanin (Jekel et al. 1988; Neuteboom et al. 1992); d and e of *Eurypelma californicum* (Schartau et al. 1983), II of *Limulus polyphemus* (Martin et al. 2007); *Androctonus australis* (Buzy et al. 1995); *Cancer magister* (Carpenter and Van Holde 1973) or CaSS2 of *Carcinus aestuarii* hemocyanin (Dolashka-Angelova et al. 2005). Sequence similarity between these respiratory proteins was assessed by their comparisons. However, the primary structures of only few representatives of hemocyanins from the subphylum crustacea, namely *Macrobrachium nipponense*, *Homarus americanus*, *P. interruptus*, *Palinurus vulgaris*, *C. magister*, and CaSS2 of *C. aestuarii*, are known (Wang et al. 2012; Kusche and Burmester 2001). Structural comparison of crustacean hemocyanin polypeptide chains by sequence alignments (Burmester 2004; Marxen et al. 2013) and immunochemistry (Markl et al. 1984) showed a discrimination between different subunit types within infraorders. High homology was found between hemocyanins from infraorder Brachyura (*Cancer magister*, *Callinectes sapidus*, *Eriocheir sinensis*). *Eriphia verrucosa*, commonly known as warty crab or yellow crab, is a species of crab infraorder Brachyura living in the Black Sea, Mediterranean Sea, and Eastern Atlantic Ocean, (Di Giamberardino 1967). Until now, there is no information about the proteins in the hemolymph of crab *E. verrucosa*. Therefore, the structure of the hemocyanin from the crab *E. verrucosa*, living in the Black Sea, is determined for the first time and compared with those of other arthropod hemocyanins.

Materials and Methods

Animals and Sample Preparation

Adult edible female *E. verrucosa* crabs were obtained from the Black Sea, Bulgaria, and maintained in a recirculating sea water system at ambient light and temperature. *E. verrucosa* hemolymph was produced using a fine gauge needle, taking care not to dislodge the fat layer on the surface and homogenized in 50 mM bicarbonate buffer (pH 7.5) in presence of a protease inhibitor cocktail (Sigma) used at tenfold of the recommended concentration. The homogenate was centrifuged (15,000g, 4 °C, 30 min), the protein-containing supernatant carefully removed, placed into a clean tube, and re-centrifuged as described above. The protein content of the supernatant was determined by Bradford assay (Bio-Rad).

Isolation and Purification

For dissociation of the aggregates, hemocyanins were dialyzed versus 50 mM bicarbonate buffer, pH 9.2, containing 2 M urea, for 24 h. The mixture was chromatographed on a Mono Q HR 16/10 column (GE Healthcare Europe GmbH), equilibrated with the same buffer, and the subunits were eluted using the same buffer and a gradient from 0.0–1.0 M NaCl. The subunits were further purified by HPLC on a Nucleosil 7C18 column (250×10 mm; Machery–Nagel, Duren, Germany) using the following conditions: eluent A, 0.1 % trifluoroacetic acid; eluent B, 80 % acetonitrile in A; gradient program: 15 % B for 5 min followed by 15–100 % B in 55 min at a flow rate of 1 ml/min. A total of 10 % SDS-polyacrylamide gel electrophoresis was carried out to analyze the purity of the subunits and their molecular masses.

Amino Acid Sequence Determinations

Automated Edman degradation was performed using N-terminal sequence analysis (Procise 494A Pulsed Liquid Protein Sequencer, Applied Biosystems GmbH, Weiterstadt, Germany). Approximately 50–200 pmol of protein was applied on the cartridge filter, previously treated with polybrene. Alignments of the obtained N-terminal amino acid sequences of EvH subunits were created by the LALING program.

MALDI-TOF Mass Spectrometry

MALDI analyses were performed using a MALDI-TOF Ultraflex II instrument (Bruker Daltonics, Bremen, Germany) operating in linear positive ion mode. Ions were formed by a pulsed UV laser beam (nitrogen laser $\lambda = 337$ nm). Five microliters of each sample (structural subunits) were mixed with 5 μ l of sinapinic acid matrix solution (saturated solution in H₂O/acetonitrile (50/50; v/v) containing 0.1 % trifluoroacetic acid). About 1 μ l of this mixture was deposited on the stainless steel sample holder. External mass calibrations were done using the Protein Calibration Standard II programme (Bruker Daltonics), based on the average values of $[M+H]^+$ of trypsinogen, protein A, bovine albumin (BSA), and the average values of $[M+2H]^{2+}$ of the same proteins at mass/charge (m/z) 23982, 44613, 66500, 22307, and 33300, respectively.

Carbohydrate Analysis

Isolated structural subunits were analyzed by orcinol–sulfuric test, where 2–4 μ l of the purified sample solutions were applied to the thin layer plate and air-dried, taking care to restrict the size of the spots to 2–3 mm in diameter. The plate was sprayed with orcinol/H₂SO₄ and heated for 20 min at 100 °C.

Isolation of Total RNA from *E. verrucosa* Hepatopancreas

Fresh samples from adult *Eriphia verrucosa* hepatopancreas tissue were fixed in a stabilization buffer (0.02 M EDTA, 0.025 M sodium citrate, 700 mg ammonium sulfate, pH 5.2) and frozen at -80°C . Total RNA was isolated with TriFast reagent (Fermentas) following the protocol of Chomczynski and Mackey (1995). Quality and concentration of the total RNA were determined by 1.2 % formaldehyde gel electrophoresis and a NanoDrop spectrophotometer, respectively. Total RNA isolation was followed by Dnase I digestion (Fermentas).

Reverse Transcription and Polymerase Chain Reaction Amplification of Hemocyanin Coding Sequence

Three-microgram total RNA, 1- μl oligo dT primer or degenerative primer F1 (TCT GCA GGA GCG TTC GAC GCG CA, Fig. 1), and nuclease-free water were mixed up to 12 μl and incubated at 65°C for 5 min. The following components were added: 1 \times 5 reaction buffer (4 μl), Ribolock RNase Inhibitor (20 u/ μl), 10 mM dNTP Mix (2 μl), revertAid H minus M-MuLV reverse transcriptase (200 u/ μl , 1 μl). The mixture was incubated at 60°C for 1 h and terminated at 70°C for 5 min (RevertAidTM H Minus First Strand cDNA Synthesis Kit, Fermentas). cDNA was diluted to 1/10, and 5 μl was subjected to PCR. The following degenerate primers were used to amplify the region encompassing a part of CuA and the complete CuB of arthropod hemocyanin site-degenerate sense “CuAI primer” corresponding to the

conserved sequence within the copper A site (5' GAACTTTTTTTTGGGTTTCATCATCAACTTAC 3') (Durstewitz and Terwilliger 1997) and a degenerate CuBR4 primer located in the CuB site as antisense (5' TGT GTT CTC TGA AGA TGT TAT CCA TGT ACT T 3').

PCR reactions were conducted in 50 μl containing 1 \times PCR buffer (Long PCR Enzyme Mix, Ferments), 4 mM MgCl_2 , 10 pmol primers, 0.2 mM dNTPs, and 2.5 units (Long PCR Enzyme Mix) on a VerityTM 9902 96-well -termed cycler under the following conditions: Denaturation at 94°C , 2 min; 35 cycles, each including denaturation at 94°C , 40 s; annealing at 55°C , 40 s, and extension at 68°C , 2 min. The final extension step was at 68°C for 5 min.

3'RACE

The 3' end of the sequence coding for *E. verrucosa* hemocyanin was obtained using the 5'/3' RACE Kit, 2nd Generation, Roche. Two-microgram total RNA from hepatopancreas was reverse transcribed, the obtained cDNA amplified with PCR anchor primer and the degenerate sense “CuAI primer” (Durstewitz and Terwilliger 1997).

The PCR reaction was carried out with 1 μl cDNA, 12, 5 μM PCR anchor primer, 12.5 μM “CuAI primer,” 0.05 mM dNTP mix, 3.5 U high fidelity taq polymerase (Roche), 5.0- μl reaction buffer with 4 mM MgCl_2 . Ten microliters of PCR product were reamplified using 12.5 μM nested CuB 3 primer (5' AAGTACATGGATAACATCTTCAGA 3') and 12.5 μM anchored primer. PCR conditions were the same as described above.

Cloning, Sequencing, and Bioinformatic Analysis

PCR products were subjected to electrophoresis on 1 % agarose gel. Clear bands were cut and purified with the Illustra GFXTM PCR DNA and gel band purification kit, GE Healthcare, and then ligated to TA cloning vector pTZ57R/T (InsTAclone PCR Cloning Kit, Fermentas). The ligation product was used to transform *E. coli* DH5 α . Universal primers M13 were used for sequencing. Sequencing was conducted on an ABI 337 sequencer. Up to 5 to 8 independent clones were sequenced to verify the authenticity. Sequencing data were analyzed by Vector NTI software.

Nucleotide and deduced amino acid sequences were compared with NCBI BLAST search programs. Additional sequences for phylogenetic analyses were retrieved from GenBank and aligned with Clustal W. The alignments of the conserved copper A- and copper B-binding site histidines were verified.

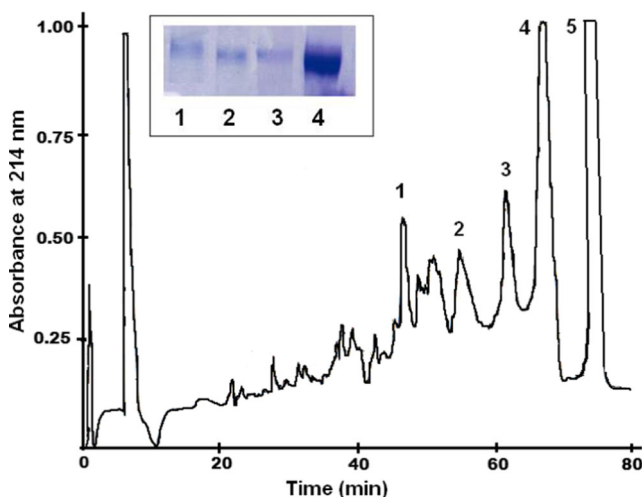


Fig. 1 Fractionation of 10 mg of *E. verrucosa* hemocyanin, chromatographed on a Mono Q HR 16/10 column (GE Healthcare Europe GmbH), equilibrated with 50 mM bicarbonate buffer, pH 9.2, containing 2 M urea. The subunits were eluted using the same buffer and a gradient from 0.0 to 1.0 M NaCl at a flow rate of 1 ml/min. *Insert* shows electrophoretic patterns of isolated fractions on a 10 % SDS gel (fraction/ peaks 1, 2, 3, and 4)

CD Measurements

Circular dichroism (CD) spectra were recorded on a J-720 dichrograph (Jasco, Tokyo, Japan). Round quartz cells with a path length of 10 mm were used in all experiments. CD spectra were recorded in the range between 200 and 250 nm with a band width of 1 nm, a scan speed of 50 nm/min, a time constant of 8.0 s, and accumulation $\times 4$. The hemocyanin solutions with $A_{280}=0.215$ were prepared in 10 mM Tris buffer (pH 7.4). The pH stability of the native molecule and structural subunit EvH4 was analyzed using buffers with pH values of the following: 11.5, 11.0, 10.0, 9.50, 9.00, 8.50, 5.72, 5.50, 5.20, 5.00, 4.50, 3.80, 3.50, and 3.00. The cocktail buffer at ionic strength 0.075 was adjusted to the given pH in the range pH 2–12: sodium citrate (pH 3.0–5.0); sodium phosphate (pH 5.0–7.0); Tris/HCl (pH 7.0–9.0); carbonate/bicarbonate (pH 9.0–10.5), and 5 M NaOH (pH 11–12).

Protein solutions were prepared in 20 mM cocktail buffer (sodium phosphate buffer, pH 7.4–5.8, sodium acetate buffer, pH 5.4–3.6, and glycine–HCl buffer, pH 3.4–1.2 in equal volumes). The final mixtures with protein concentrations of 20 μ M were incubated for 20 min at room temperature before optical measurements. Each spectrum was the average of four scans, and the results are expressed as mean residue ellipticity (MRE, $[\Theta]_{222}$) in $\text{deg cm}^2 \text{dmol}^{-1}$.

Results and Discussion

Isolation of *Eriphia verrucosa* Hemocyanin and its Isoforms

The crab *E. verrucosa* lives in the Black Sea, Mediterranean Sea, and Eastern Atlantic Ocean at different environments and conditions. The hemolymph was obtained from the yellow crab *E. verrucosa*, collected from the Black Sea, and after centrifugation at 15,000g, 4 °C for 30 min, the native hemocyanin was purified by gel filtration chromatography on a Superdex column. One main peak was eluted from the column by 50 mM bicarbonate buffer (pH 7.5), and after additional purification of 3 mg of this fraction by HPLC on a Nucleosil 7C18 column, its N-terminal sequence was determined. Determination of 16 amino acids (ADSADVALAQKQHVDN-) from the N-terminus by Edman degradation confirmed the *E. verrucosa* hemocyanin (EvH) aggregates for the purified fractions.

After dissociation of the obtained *E. verrucosa* hemocyanin by dialysis versus 50 mM bicarbonate buffer, pH 9.2 and 2 M urea for 24 h, of the obtained *E. verrucosa* hemocyanin on a Superdex column, five fractions were eluted on a Mono Q HR column with a linear gradient from 0.1–1.0 M NaCl in 50 mM bicarbonate buffer, pH 9.6 (Fig. 1). The obtained fractions were desalted by gel filtration through a Sephadex G-25 (Pharmacia)

column, and electrophoretic analysis confirmed a high-grade separation of four structural subunits (fractions 1–4) with molecular masses of 70–75 kDa (Fig. 1, insert). From the eluted fractions, number 5 is a non-dissociated hemocyanin; therefore, only fractions 1–4 were additionally analyzed. The subunits and molecular weight markers were applied to gel-exclusion chromatography (2 \times 150-cm SuperdexTM 200 column) and eluted with 0.1 M Tris–HCl, pH 8.2, 5 mM CaCl_2 , 5 mM MgCl_2 at a flow rate of 9 ml/h. The weight-average molecular masses of the subunits were determined to be in the range of about 75 kDa, according to the elution profile of the markers.

To determine more precise the molecular masses of the isolated subunits from *E. verrucosa* and their N-terminal sequences, more precisely fractions 1, 2, 3, and 4 were additionally purified on a Nucleosil 100 RP-18 column, where only one main peak was eluted from the column (Fig. 2). Then, the masses of the polypeptides in each fraction were determined with more precision by MALDI-TOF. Figure 3 shows the MALDI spectrum of fraction 1 (Fig. 1) for which a molecular mass of 75 098.62 Da was determined (Fig. 3). The masses of the other 3 subunits were found to be in the same region 74, 488 Da (EvH2), 75,753 Da (EvH3), and 74,713 Da (EvH4), correlating with the masses from other arthropod hemocyanins (Burmester 1996).

The N-terminal sequences of the purified subunits were determined by Edman degradation, and the obtained results are compared in Fig. 4 with those of other arthropod hemocyanin subunits. A high similarity score was found between N-terminal sequences of hemocyanin subunits from *Eriphia verrucosa* (EvH1, EvH3) and polypeptide chains from hemocyanins found in other species. Comparison of the N-terminal sequences of EvH1, EvH2, EvH3, and EvH4, with those of *C. magister* and *C. aestuarii* of infraorder Brachyura, shows conserved Asp and Ser residues at positions 2 and 3,

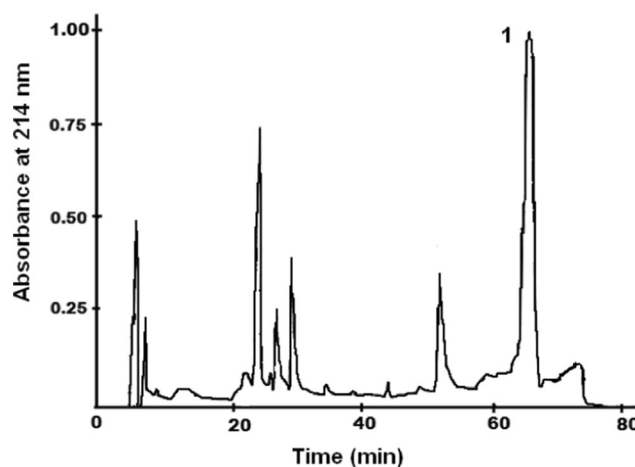
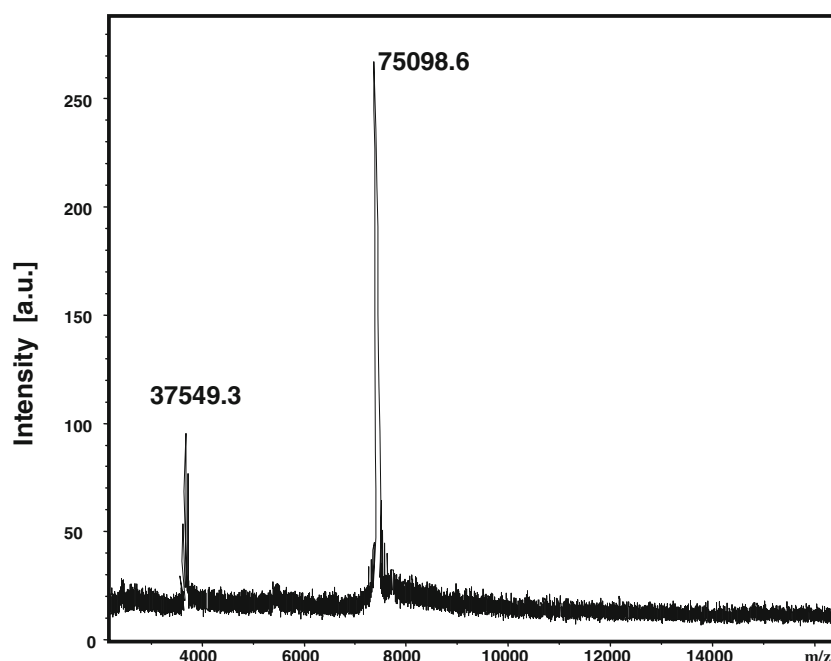


Fig. 2 HPLC purification of structural subunits on a Nucleosil 7 C18 column (250 \times 10 mm; Machery–Nagel, Düren, Germany) using the following conditions: eluent A, 0.1 % trifluoroacetic acid; eluent B, 80 % acetonitrile in A; gradient program, 15 % B for 5, followed by 15–100 % B in 55 min at a flow rate of 1 ml/min

Fig. 3 MALDI spectrum of structural subunit 1 from *E. verrucosa* Hc isolated on a Mono Q HR 16/10 column, followed by additional purification on a Nucleosil RP C18 column (Fig. 2). The sample was measured by MALDI-TOF Ultraflex II (Bruker Daltonics, Bremen, Germany)



respectively. Gly5 and Gly6 are also conserved in EvH3, Cp1, Cm3, Cm6, and CaSS2. Predominant Ala, Gln, Lys, Gln, as well as Asp and Ser residues were observed in most of the subunits in positions 10, 11, 12, 13, 15, and 18. Within the infraorder Brachyura, the positions 16 (Val) and 17 (Asp) are conserved with Val and Asp residues, respectively.

High similarity scores were found comparing the N-terminal sequences of subunit 3 from *E. verrucosa* (EvH3) with those of *C. pagurus* (Cp1), *C. magister* (Cm3 and Cm6), and *C. aestuarii* (CaSS2). Therefore, these five subunits were considered to be closely related.

Isolation of a Partial Hemocyanin cDNA Sequence (EvH)

Hemocyanin sequences were initially amplified with degenerate crustacean hemocyanin primers based on the conserved regions of copper A and copper B binding sites.

Crustaceae species, Infraorder - Brachyura																			
	1			5					10					15				20	
EvH1	A	D	S	-	A	D	V	A	L	A	Q	K	Q	H	D	V	N		
EvH2					A	V	K	S	L	-	Q	Q	Q	F	D	V	N	S	L
EvH3		D	S	P	G	G		F	D	A	Q	K	Q	H	D	V	N		
EvH4									L	A	Q	K	Q	F	D	V	N	S	X
CmH1	X	D	-	P	A	S	V	S	D	A	X	K	Q						
CmH2						T	C	L	A	H	K	Q	Q	A	V	N	R	L	L
CmH3		D	S	P	G	G	A	S	D	A	Q	K	Q	H	D	V	N	S	I
CmH4					G	F	G	E	D	I	A	M	K	Q	H	Q	V	N	S
CmH6			T	A	G	G	A	F	D	A	Q	K	Q	H	D	V	N	S	A
CaSS2		D	S	P	G	G	A	S	D	A	Q	K	T	F	D	V	N	S	L

Fig. 4 The relationship between N-terminal sequences of structural subunits originating from *E. verrucosa* (Black Sea; EvH1-4), *Cancer magister* (Cm 1, 2, 3, 4, and 6), and *Carcinus aestuarii* (CaSS2)

Amplification resulted in a 540-bp product that was cloned and sequenced. The sequence was used to design additional primers to further amplify hemocyanin following the 3' RACE protocol (ROCHE). Using PCR with anchor primer (ROCHE), "CuAI primer" and the nested CuBF3 specific primer (Fig. 5a), a 1.022-kb cDNA fragment was amplified, cloned, and sequenced. The identical overlapping (35 bases) of both fragments, 540 bp and 1.022 kb, allowed their correct assembling. The obtained contig (1523 bp) covering about 2/3 of the putative *Hc* gene contains ORF of a 1309 bp, 3'UTR region (201 bp), and polyA tail (13 bp) (data not shown).

The translated amino acid sequence (435 AA in length) showed 70; 83; 84, and 81 % identity with the *C. magister* hemocyanin subunits 3 (AAW57891.1), 4 (AAW57892.1), 5 (AAW57893.1), and 6 (AAA96966.2), respectively (Fig. 5b). High identity (65 %) was also observed between EvH and CaSS2 of *C. aestuarii* (P 84293.1), *Callinectes sapidus* (AF249297.1) (78 %), and *Eriocheir sinensis* (AEG64817.1) (74 %).

These values are very close to the homology reported between the subunits of other hemocyanins, and we may suggest that this fragment belongs to EvH4 or EvH5.

There is a vast amount of data supporting the hypothesis that arthropod hemocyanins consist of three domains (Hazes et al. 1993; Decker and Jaenicke 2004; Terwilliger et al. 2006). Crystallographic studies of hemocyanin from *Panulirus* and *Limulus* (Volbeda and Hol 1989; Hazes et al. 1993) have shown that arthropod hemocyanins consist of three structural domains. The region between residues 220 and 394 in domain 2 is the most conserved and contains the oxygen-binding CuA and CuB sites. Each copper ion is ligated to three histidine side chains. The six histidines marked by

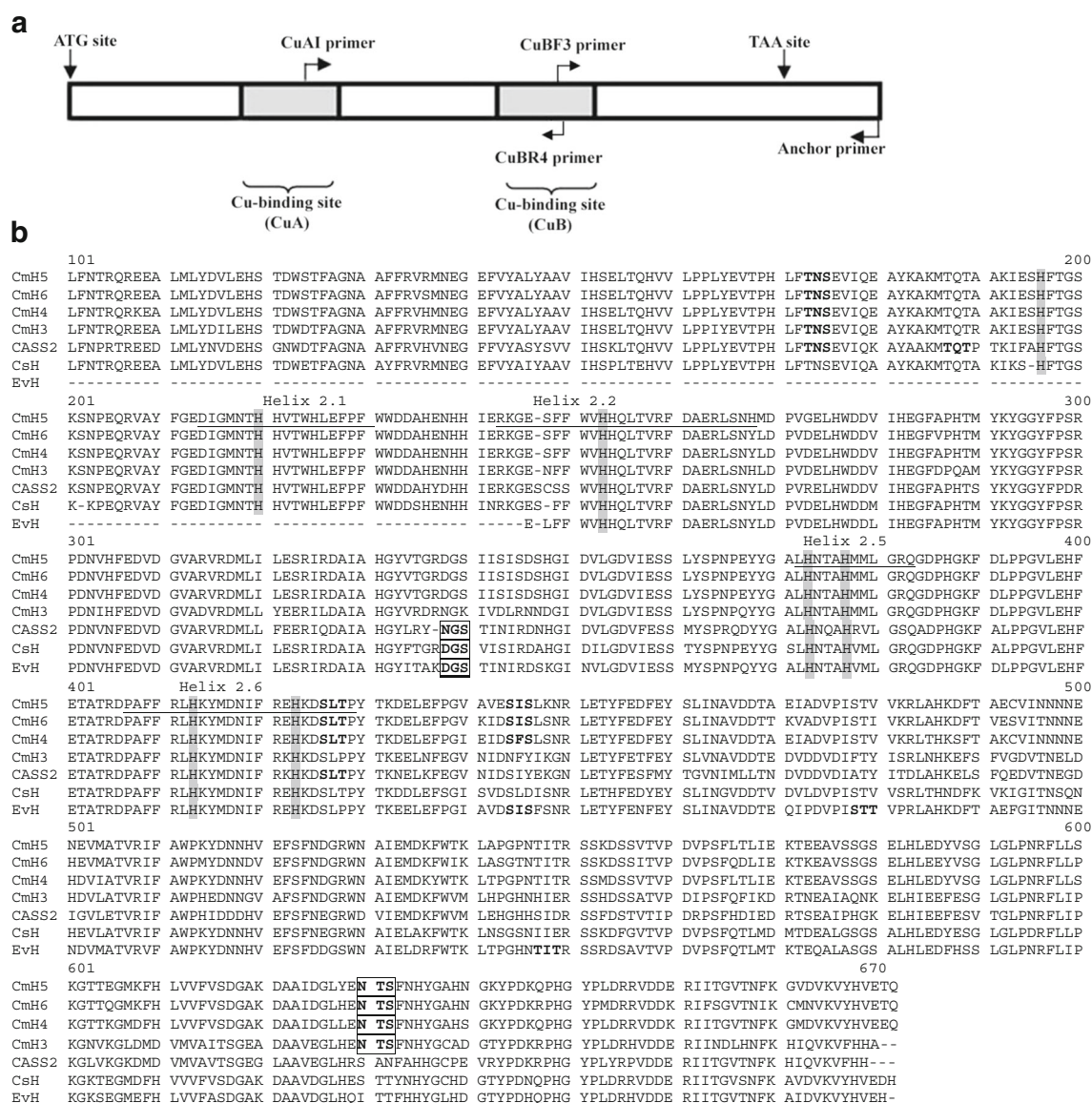


Fig. 5 **a** Schematic presentation of primer positions: PCR anchor primer (ROCHE), “CuAI primer”—specific for the CuA binding site region and CuBF3-nested primer; **b** alignment between partial hemocyanin amino acid sequences, subunits from *E. verrucosa* (EvH), *C. magister* CmH 3 (AAW57891.1), 4 (AAW57892.1), 5 (AAW57893.1), 6 (AAA96966.2),

Callinectes sapidus (AAF64305.1), and *C. aestuarii* (CaSS2; P84293.1). Borders of the helices and CuA and CuB regions are underlined. Cubinding histidines are shown in gray color; the positions of N-glycosylated sites are given in boxes while the putative O-glycosylated sites are bolded

gray color in Fig. 5b are implicated in Cu binding according to their highly conserved character among arthropod hemocyanin subunits (Durstewitz and Terwilliger 1997; Dolashka-Angelova et al. 2005). The Cu binding histidines are located at positions 196, 220, 253, 373, 377, 413, and 423 in EvH and all hemocyanins, studied here (Fig. 5b). The high conservation of the histidine ligands launch the hypothesis that the isolated cDNA is a gene encoding a protein that binds Cu. The CuA helix pair in *E. verrucosa* subunit extends from residue 214 to residue 230 and from residue 243 to residue 268 indicating that His253 of EvH, CaSS2, CmH5, and CmH6 is involved in oxygen-binding CuA. The histidine residues binding the

copper ion at the CuB site are located at positions 373, 377, 413, and 423 (Fig. 5b).

Glycosylation of Structural Subunits of *E. verrucosa* Hemocyanin

It is known that mollusk and arthropod Hcs are glycosylated, but the glycans represent only about 1–2 % of the protein masses of arthropod Hcs, e.g., for *C. aestuarii* hemocyanin (CaSS2), 1.6 % could be determined (Dolashka-Angelova et al. 2001, 2005; Kostadinova et al. 2013). To identify the glycosylated subunits, the orcinol–sulfuric test was applied to

four subunits EvH1-4 and native molecule of EvH and compared with the result on glycosylated subunit CaSS2 of *C. aestuarii* hemocyanin (Dolashka-Angelova et al. 2005). No glycans were identified in subunit 4, but the test demonstrates that subunits 1, 2, and 3 are glycosylated (Fig. 6). Moreover, the spots on positions 1 and 3 are less intense compared to the position 2 indicating a higher sugar content for subunit 2, which, however, is of lower intensity than for position 6, the spot for glycosylated CaSS2.

Three consensus sequences for O-glycosylation and one for N-glycosylation were identified in CaSS2 after trypsin digestion, separation of glycopeptides, and amino acid sequencing (Dolashka-Angelova et al. 2001, 2005). One putative N-linked site was observed at positions 338–340 in CaSS2 with a consensus sequence Asn-Gly-Ser, typical for N-glycosylation. However, as is shown in Fig. 5b, Asn residues are substituted by Asp at the same position in EvH and CmH 4, 5, and 6 confirming that these subunits can not be N-glycosylated. The absence of N-glycosylation sites (NX(T/S)) in the short part of the primary structure of EvH shows that this subunit is not glycosylated. The putative N-glycosylation sites marked by boxes are located at positions 630–632 in *C. magister* subunits 3, 4, 5, and 6 (Fig. 5b). One putative N-linkage site was also identified at position 166 in *P. elephas* α -type subunits 1, 2, and 3 (Meissner et al. 2003), and β -type subunit a, b at position 470 in *P. interruptus*. Four potential N-glycosylation sites are present in each of the *H. americanus* pseudohemocyanin (Burmester 1999). No carbohydrate moiety was detected in native *E. californicum* Hc, and its seven subunits which fits to the observation that chelicerate hemocyanins are synthesized in the cytosol and not by the rough ER as known for crustacean hemocyanins (Voit et al. 2000).

Instead of N-linkage sites, three putative O-linkage sites were identified in EvH which suppose glycosylation at positions 444–446, 478–480, and 547–549 (Fig. 5b). Several other O-glycosylation sites were published for CaSS2 at positions 73–75, 83–85, 198–200, 426–428 (Dolashka-Angelova et al. 2005), but their positions do not correlate with the putative glycosylated sites in EvH.

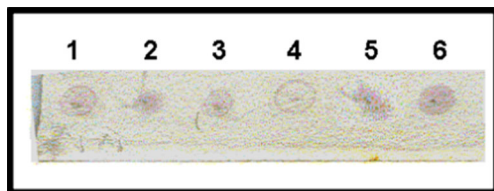


Fig. 6 Orcinol-sulfuric acid test of (glyco) subunits eluted by HPLC and applied on to a silica-gel plate. The spots on positions: position 1—EvH1; position 2—EvH2; position 3—EvH3; position 4—EvH4; position 5—EvH; position 6—CaSS2

Stability of *E. verrucosa* Hemocyanin

There are several reports on the biophysical and structural properties of the function and stability of molluscan and arthropod Hcs (Ali et al. 2000; Coates et al. 2012; Coates and Naim 2014; Spinozzi et al. 2005).

The conformational stability of the native aggregates of several arthropod Hcs and their isolated structural subunits toward various denaturants (pH and guanidine hydrochloride (Gdn-HCl)) indicate that hydrophilic and polar forces stabilize

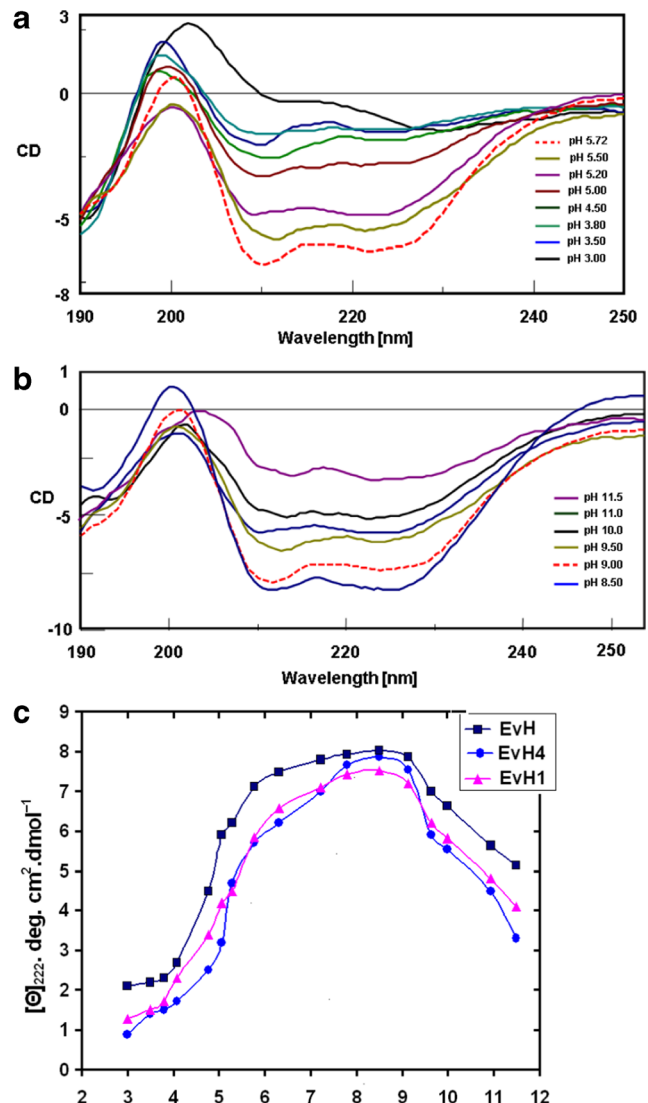


Fig. 7 **a** pH stability of structural subunit EvH4 analyzed by circular dichroism (CD). Spectra at pH values 5.72, 5.50, 5.20, 5.00, 4.50, 3.80, 3.50, and 3.00 and **b** at pH values 11.5, 11.0, 10.0, 9.50, 9.00, and pH 8.50. Spectra were recorded on a J-720 dichrograph (Jasco, Tokyo, Japan) in the range between 200 and 250 nm with a band width of 1 nm, a scan speed of 50 nm/min, a time constant of 8.0 s, and accumulation -4. The hemocyanin solutions with $A_{280}=0.215$ were prepared in different buffers. **c** Influence of pH on $[\theta]_{222}$ of native CpH and two structural subunits nonglycosylated EvH4 and glycosylated EvH1 at different pH values (3.0–11.5)

the quaternary structure (Hristova et al. 1997; Dolashka-Angelova et al. 1999, 2000). The reassociation behavior of arthropodan hemocyanin *Carcinus maenas* was analyzed by ESI-MS (Bruneaux et al. 2009). By returning to a more neutral pH after dissociation of the native *C. maenas*, a complete reassociation was not observed.

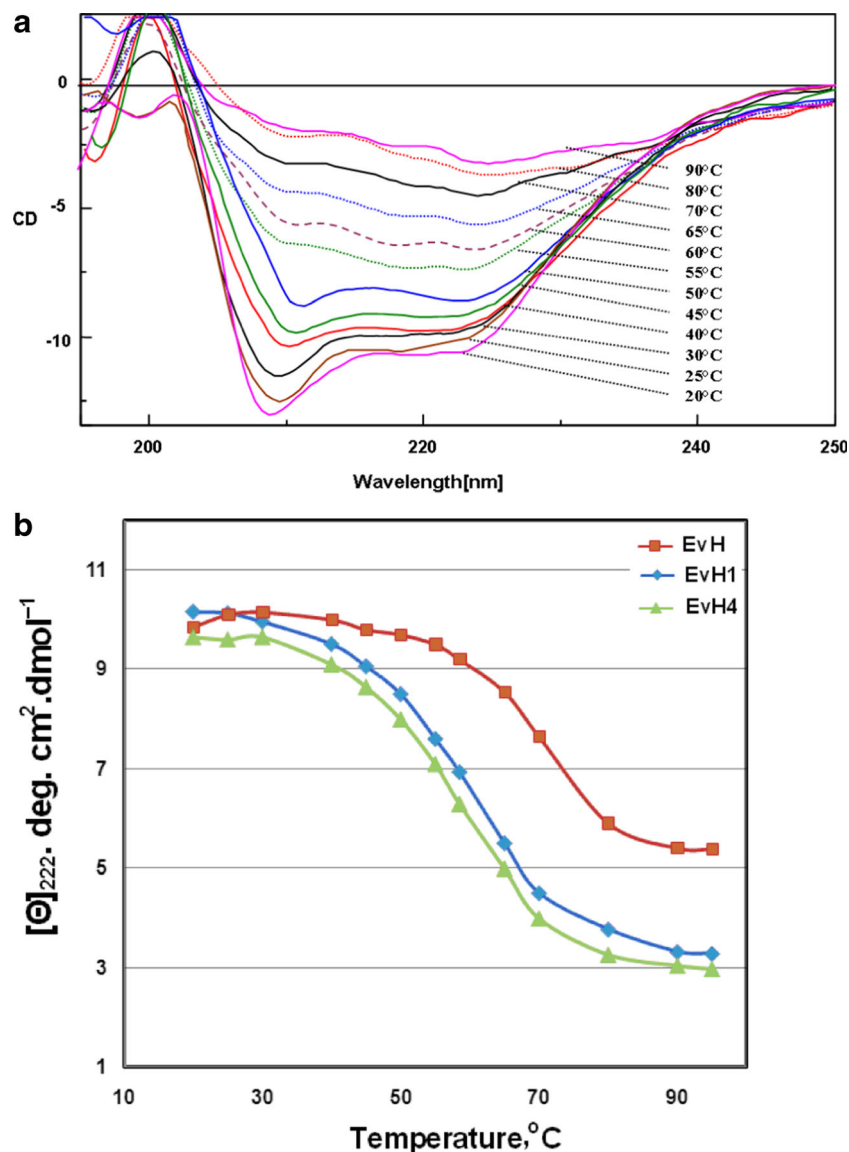
Changes in the secondary structure of native EvH and two structural subunits (glycosylated EvH1 and nonglycosylated EvH4) at different pH values (3.0–11.5) were followed by near UV-CD measurements of $[\theta]_{222}$ in the region between 200 and 250 nm. The far-UV CD spectra of the native protein and two structural subunits in 50 mM Tris/HCl, pH 8.2, are dominated by a negative dichroic band with two minima at 210 and 220 nm (Fig. 7a, b).

Figure 7c shows that the $[\theta]_{222}$ vs pH plots represent denaturation studies of the native molecule and two structural subunits, EvH1 and EvH4, of *E. verrucosa* hemocyanin by pH.

The curve indicates that the denaturation process of the native molecule in the alkaline region represents dissociation of the native molecule into its structural subunits at pH values over 9.0 followed by their denaturation at higher pH values. However, it may be difficult to distinguish between the effects on the quaternary structure of the oligomeric protein (initial dissociation) and those on the tertiary and secondary structure (i.e., subunit unfolding).

Comparison of the pH dependence of the dichroic curves of the native molecule with those of two structural subunits ($[\theta]_{222}$ vs (pH)) at low and high pH values at 25 °C shows a similar behavior for all 3 proteins. The $[\theta]_{222}$ /pH values are

Fig. 8 **a** Temperature stability of structural subunit EvH1 and EvH4 of *E. verrucosa* hemocyanin ($A_{280}=0.274$) analyzed by circular dichroism (CD). Spectra were recorded at 20–90 °C in the range between 200 and 250 nm. **b** Temperature dependence of the ellipticity $[\theta]_{222}$ at 222 nm of native EvH in 50 mM Tris–HCl, buffer, containing 5 mM CaCl_2 , 5 mM MgCl_2 , at pH 8.2 and structural subunits EvH1 and EvH4



more or less independent from pH within the pH range 6.0–9.2 for native EvH, but for both subunits, the constant pH range is shortened to 7.5–9.0 (Fig. 7c). These data confirm that the native EvH is more stable to pH denaturation as compared to its structural subunits EvH1 and EvH4. No influence of glycosylation was observed in EvH1. In the alkaline part (pH 8–11.5), relative changes are too small and non-cooperative (within a wide pH interval), indicating that for alkaline denaturation of EvH, EvH4, and EvH1 as a reversible process cannot be achieved.

Figure 8a shows the CD spectra of the native molecule of EvH in 50 mM Tris–HCl, buffer, containing 5 mM CaCl_2 , 5 mM MgCl_2 , at pH 8.2, recorded in the temperature interval 20–90 °C. The temperature dependence of the ellipticity at 222 nm of the native molecule and the structural subunits EvH1 and EvH4 show that the thermal denaturation of the EvH is also in reversible process (Fig. 8b). The thermostability of EvH and its subunits were compared by their melting temperatures, T_m , the midpoint in the sigmoidal denaturation curves. The melting temperature for the native EvH ($T_m = 72$ °C) is larger compared to its structural subunits EvH1 ($T_m = 60$ °C) and EvH4 ($T_m = 57$ °C) and correlates with thermostability of arthropod hemocyanins *C. aestuarii* (T_m 72 °C), *Callinectes sapidus* ($T_m \sim 76$ °C), and *Maia squinado* ($T_m \sim 72$ °C) (Dolashka-Angelova et al. 1999, 2000). The larger T_m values found for native EvH compared to its subunits EvH1 and EvH4 is an excellent indication for a stabilization of the protein caused by oligomerization.

Conclusion

In this study, we report for the first time information about the hemocyanin of the marine crab *Eriphia verrucosa* living in the Black Sea. Hemocyanin was isolated and purified from the hemolymph, and four structural subunits (EvH1, EvH2, EvH3, and EvH4) with molecular masses in the range of least 75–76 kDa were identified. Its isolated partial hemocyanin cDNA (1523 bp) corresponds to the region encompassing part of the conservative CuA, the full CuB binding sites, and the 3' end of the gene. The alignment shows a high degree of sequence similarity of EvH with those of *C. magister*, *C. aestuarii*, *C. sapidus*, and *E. sinensis* hemocyanins which suggests a common structure. Three of the EvH subunits (EvH1, EvH2, and EvH3) are glycosylated as confirmed by the orcinol–sulfuric test. Several putative O-linkage sites were found in the identified amino acid sequence of EvH.

In this paper, we present communication for the first time some preliminary results on the pH- and thermostability of the native protein and its structural subunits EvH1 and EvH4, as characterized by CD measurements. We report on the pH values under which reversible structural changes of EvH, EvH1, and EvH4 can exist and strong alkaline as well as acid

environment causes changes in quaternary and secondary structure.

Acknowledgments This work was supported by Bulgarian Ministry of Education, projects DHRC /01/6 and “Young researchers” DMU 03/26, Deutsche Forschungsgemeinschaft (DFG-STE 1819/5-1/2012), Germany, grant no. BG051PO001-3.3.06-0025, financed by the European Social Fund and Operational Programme Human Resources Development (2007–2013) and co-financed by Bulgarian Ministry of Education, Youth and Science.

References

- Ali S, Abbasi A, Stoeva S, Kaye R, Dolashka-Angelova P, Schwarz H, Voelter W (2000) Oxygen transport proteins: III. Structural studies of the scorpion *Buthus indicus* hemocyanin, partial primary structure of its subunit Bsin1. *Comp Biochem Physiol B* 126:361–376
- Bruneaux M, Terrier P, Leize E, Mary J, Lallier FH, Zal F (2009) Structural study of *Carcinus maenas* hemocyanin by native ESI-MS: interaction with L-lactate and divalent cations. *Proteins* 77(3): 589–601
- Burmester T (1996) Molecular evolution of the arthropod hemocyanin superfamily. *Mol Biol* 18:184–195
- Burmester T (1999) Identification, molecular cloning and phylogenetic analysis of a nonrespiratory pseudo-hemocyanin of *Homarus americanus*. *J Biol Chem* 274:13217–13222
- Burmester T (2004) Evolutionary history and diversity of arthropod hemocyanins. *Micron* 35:121–122
- Buzy A, Gagnon J, Lamy J, Thibault P, Forest E, Hudry-Clergeon G (1995) Complete amino acid sequence of the Aa6 subunit of the scorpion *Androctonus australis* hemocyanin determined by Edman degradation and mass spectrometry. *Eur J Biochem* 233:93–101
- Carpenter D, van Holde K (1973) Amino acid composition, amino-terminal analysis, and subunit structure of *Cancer magister* hemocyanin. *Biochemistry* 12:2231–2238
- Chen HY, Ho SH, Soong K, Chen IM, Cheng JH (2007) Identification of a female-specific hemocyanin in the mud crab, *Scylla olivacea* (Crustacea: Portunidae). *Zool Stud* 46:194–202
- Chomczynski P, Mackey K (1995) Substitution of chloroform by bromochloropropane in the single-step method of RNA isolation. *Anal Biochem* 225:163–164
- Coates J, Nairn J (2014) Diverse immune functions of hemocyanins. *Dev Comp Immunol* 45:43–55
- Coates CJ, Whalley T, Nairn J (2012) Phagocytic activity of *Limulus polyphemus* amebocytes in vitro. *J Invertebr Pathol* 111(3):205–210
- Cong Y, Zhang Q, Woolford D, Schweikardt T, Khant H, Dougherty M, Ludtke SJ, Chiu W, Decker H (2009) Structural mechanism of SDS-induced enzyme activity of scorpion hemocyanin revealed by electron cryomicroscopy. *Structure* 17:749–758
- Decker H, Jaenicke E (2004) Recent findings on phenoloxidase activity and antimicrobial activity of hemocyanins. *Dev Comp Immunol* 28: 673–687
- Di Giamberardino L (1967) Dissociation of *Eriphia* hemocyanin. *Arch Biochem Biophys* 118:273–278
- Dolashka-Angelova P, Hristova R, Stoeva S, Voelter W (1999) Spectroscopic properties of *Carcinus aestuarii* hemocyanin and its structural subunits. *Spectrochim Acta Part A* 55:2927–2934
- Dolashka-Angelova P, Stoeva S, Hristova R, Schuetz J, Voelter W (2000) Structural and spectroscopic studies of the native hemocyanin from *Maia squinado* and its structural subunits. *Spectrochim Acta A* 56: 1985–1999

- Dolashka-Angelova P, Beltramini M, Dolashki A, Salvato B, Voelter V (2001) Carbohydrate composition of *Carcinus aestuarii* hemocyanin. Arch Biochem Biophys 389:153–158
- Dolashka-Angelova P, Dolashki A, Savvides SN, Hristova R, Van Beeumen J, Voelter W, Devreese B, Weser U, Di Muro P, Salvato B, Stevanovic S (2005) Structure of hemocyanin subunit CaeSS2 of the crustacean Mediterranean crab *Carcinus aestuarii*. J Biochem 138:303–312
- Durstewitz G, Terwilliger NB (1997) cDNA cloning of a developmentally regulated hemocyanin in the crustacean *Cancer magister* and phylogenetic analysis of the hemocyanin gene family. Mol Biol Evol 14:266–276
- Hagner-Holler S, Schoen A, Erker W, Marden JH, Rupprecht R, Decker H, Burmester T (2004) A respiratory hemocyanin from an insect. Proc Natl Acad Sci 101:871–874
- Hazes B, Magnus KA, Bonaventura C, Bonaventura J, Dauter Z, Kalk KH, Holx WG (1993) Crystal structure of deoxygenated *Limulus polyphemus* subunit II hemocyanin at 2.18 Å resolution: clues for a mechanism for allosteric regulation. Protein Sci 2:597–619
- Herskovits TT (1988) Recent aspects of the subunit organization and dissociation of hemocyanins. Comp Biochem Physiol B 91:597–611
- Hristova R, Dolashka P, Stoeva S, Voelter W, Salvato B, Genov N (1997) Spectroscopic properties and stability of hemocyanins. Spectrochim Acta A 53:471–478
- Jaenicke E, Pairet B, Hartmann H, Decker H (2012) Crystallization and preliminary analysis of crystals of the 24-meric hemocyanin of the emperor scorpion (*Pandinus imperator*). PLoS ONE. doi:10.1371/journal.pone.0032548
- Jekel PA, Bak HJ, Soeter NM, Vereijken JM, Beintema JJ (1988) *Panulirus interruptus* hemocyanin. The amino acid sequence of subunit b and anomalous behaviour of subunits a and b on polyacrylamide gel electrophoresis in the presence of SDS. Eur J Biochem 178:403–412
- Kölsch A, Hörnemann J, Wengenroth C, Hellmann N (2013) Differential regulation of hexameric and dodecameric hemocyanin from *A. leptodactylus*. Biochim Biophys Acta 1834:1853–1859
- Kostadinova E, Dolashka P, Velkova L, Dolashki A, Stevanovic S, Voelter W (2013) Positions of the glycans in molluscan hemocyanin, determined by fluorescence spectroscopy. J Fluoresc 23:753–760
- Kusche K, Burmester T (2001) Molecular cloning and evolution of lobster hemocyanin. Biochem Biophys Res Commun 282:887–892
- Markl J, Gebauer W, Runzler R, Avissar I (1984) Immunological correspondence between arthropod hemocyanin subunits. I. Scorpion (*Leiurus, Androctonus*) and spider (*Eurypelma, Cupiennius*) hemocyanin. Hoppe Seylers Z Physiol Chem 365:619–631
- Martin A, Depoix F, Stohr M, Meissner U, Hagner-Holler S, Hammouti K (2007) *Limulus polyphemus* hemocyanin: 10 Å structure, sequence analysis, molecular modelling and rigid-body fitting reveal the interfaces between the eight hexamers. J Mol Biol 366:1332–1350
- Marxen JC, Pick C, Kwiatkowski M, Burmester T (2013) Molecular characterization and evolution of haemocyanin from the two freshwater shrimps *Caridina multidentata* (Stimpson, 1860) and *Atyopsis moluccensis* (De Haan, 1849). J Comp Physiol B 183:613–624
- Meissner U, Stohr M, Kusche K, Burmester T, Stark H, Orlova EV, Markl J (2003) Quaternary structure of the European spiny lobster *Palinurus elephas* 1x6-mer hemocyanin from cryoEM and amino acid sequence data. J Mol Biol 325:99–109
- Mičetić I, Losasso C, Di Muro P, Tognon G, Benedetti P, Beltramini M (2010) Solution structures of 2x6-meric and 4x6-meric hemocyanins of crustaceans *Carcinus aestuarii*, *Squilla mantis* and *Upogebia pusilla*. J Struct Biol 171:1–10
- Neuteboom B, Jekel PA, Beintema JJ (1992) Primary structure of hemocyanin subunit c from *Panulirus interruptus*. Eur J Biochem 206:243–249
- Sánchez D, Ganfornina MD, Gutierrez G, Bastani MJ (1998) Molecular characterization and phylogenetic relationship of a protein with potential oxygen-binding capabilities in the grasshopper embryo. A hemocyanin in insects? Mol Biol Evol 15:415–426
- Schartau W, Eyerle F, Reisinger P, Geisert H, Storz H, Linzen B (1983) Hemocyanins in spiders. XIX. Complete amino-acid sequence of subunit d from *Eurypelma californicum* hemocyanin, and comparison to chain e. Hoppe Seyler Z Physiol Chem 364:1383–1409
- Spinozzi F, Gatto S, De Filippis V, Carsughi F, Di Muro P, Beltramini M (2005) Contribution of the copper ions in the dinuclear active site to the stability of *Carcinus aestuarii* hemocyanin. Arch Biochem Biophys 439:42–52
- Terwilliger NB, Ryan M, Phillips MR (2006) Crustacean hemocyanin gene family and microarray studies of expression change during eco-physiological stress. Integr Comp Biol 46:991–999
- Van Holde KE, Miller KI (1995) Hemocyanins. Adv Protein Chem 47:1–81
- Voit R, Feldmaier-Fuchs G, Schweikardt T, Decker H, Burmester T (2000) Complete sequence of the 24-mer hemocyanin of the tarantula *Eurypelma californicum*. Structure and intramolecular evolution of the subunits. J Biol Chem 275:39339–39344
- Volbeda A, Hol WG (1989) Crystal structure of hexameric haemocyanin from *Panulirus interruptus* refined at 3.2 Å resolution. J Mol Biol 209:249–279
- Wang W, Xia X, Liu F, Chen X, Yang H, Ning Q (2012) Cloning and characterization of the hemocyanin gene of prawn *Macrobrachium nipponense*. Turk J Biochem 37:348–355